

Shock wave study of kinetics of carbon particle charging

A. Emelianov^{1*}, A. Eremin¹, H. Jander², S. Bronin¹, A. Khrapak¹

¹Joint Institute for High Temperatures, Russian Academy of Sciences, Moscow, Russia

²Institut für Physikalische Chemie, Universität Göttingen, Germany

Abstract

The processes of electrical charging of carbon nanoparticles formed during shock wave pyrolysis of carbon suboxide C_3O_2 are studied. Experiments performed in the mixtures of Ar + (0 – 2)% C_3O_2 have shown that the electron and light ion concentrations, originating from the natural sodium admixture in shock-heated gas, are significantly modified in the presence of carbon particles. To analyze the observed processes the kinetics of the stepwise sodium ionization and following recombination of free electrons and sodium ions on the particle surface has been considered.

Introduction

It is well known that the ionization of gases and soot particles has a significant role in the process of combustion of hydrocarbon fuels. The negative and positive charged soot particles were observed and studied in flames [1-5] and in low temperature plasma of combustion products [6]. However, there is only one work [7] which refers to the ionization of soot particles in the shock wave. In the papers [2,8,9] the ionic and nonionic mechanisms of formation of soot in flames has been discussed. Recent simulations of the charging of soot in flames [10,11] did not reveal significant influence of charged particles in the formation of soot. In these works the various possible mechanisms of ion formation in flames are discussed and it is stated that the chemi-ionization mechanism is responsible for the abnormally high concentration of ions in flames. However, in [10,11] the admixtures of alkali metal as an additional source of electrons were not considered. On the other hand, it is known that in the presence of typical atmospheric concentrations of alkali metals (10^{12} – 10^{13} cm^{-3} [12-15]) soot becomes charged even at temperatures of ~ 2000 K. One of the first investigations of the influence of alkali metals on the charging of soot particles and their growth in premixed flames was performed in [1]. In flames, however, the kinetics of particle charging can not be investigated. Therefore, in the present work for a study of kinetics of nanoparticle charging the experiments in the shock heated gases have been selected.

Specific Objectives

The purpose of this work is to observe the charging of carbon particles formed during pyrolysis of C_3O_2 in a shock tube at different temperatures and concentrations. It continues the series of investigations of kinetics of soot and hydrogen free carbon particle formation during shock-wave pyrolysis of various carbon-bearing species [16-19]. An advantage of using C_3O_2 as a soot precursor is the lack of PAH that allows to neglect chemi-ionization processes and to consider thermo-ionization processes only. Investigations of complex plasma-

particle systems, which have been actively studied during the last years [20-22] were quite helpful and gave information for a qualitative analysis of the observed data. The results of the present analysis is useful for the understanding and control of coagulation and removal of soot particles in the combustion processes.

Results and Discussion

Experimental set-up

Experiments in a high pressure shock tube of 70 mm inner diameter and a 4.5 m long driver section were carried out. The installation has been described elsewhere [16,17]. Test experiments were performed in pure argon. Particle charging was then investigated in mixtures initially consisting of 0.05 – 2% C_3O_2 in Ar.

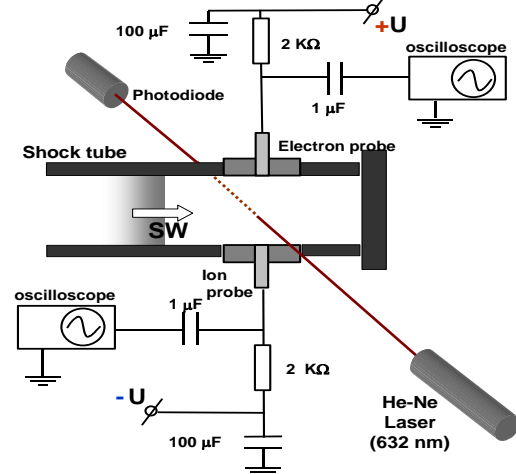


Fig. 1. Experimental set up and the diagnostic equipment.

The temperatures T_5 and pressures P_5 behind the reflected shock wave were varied in the range of 2000 – 3600 K and 15 – 30 bar.

Process of propagation of the incident and reflected shock waves and the following growth of carbon nanoparticles was observed by means of laser extinction measurements at the wavelength 633 nm. The time

* Corresponding author: aemelia@ihed.ras.ru

resolution of these measurements was $(1 - 2) \times 10^{-6}$ s. For the measurements of the concentrations of free electrons and ions the shock tube was equipped with two sensitive electric Langmuir probes. The diameter of each probe was 6 mm, the electric voltage on the probes could be changed in the ± 80 V range. In Fig. 1 the scheme of the experimental set up and the diagnostic equipment are shown.

Probe calibration method

For the absolute calibration of the probes additional experiments were carried out in argon with known impurities of sodium (mainly as a sodium chloride NaCl). According to [12-15], the natural contents of sodium chloride in the majority of gases (argon, nitrogen, air) is rather stable and equal to $(2 \pm 1) \cdot 10^{-5}$ %. In Fig. 2 the characteristic profile of the signal on the electron probe ΔU with a voltage of $U = +50$ V together with the pressure signal at $T_5 = 2380$ K and $P_5 = 25$ bar is shown.

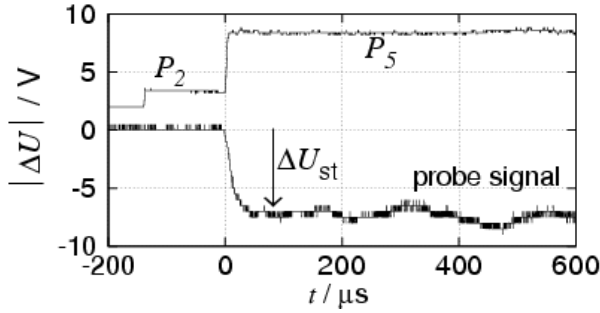


Fig. 2. An example of pressure and probe signals behind shock wave in Ar ($P_5 = 25$ bar, $T_5 = 2380$ K).

The rise time of the signal of $\sim 3 \times 10^{-5}$ s agrees with previous data of sodium ionization behind shock waves [14,23,24]. According to [23] NaCl first dissociates to $\text{Na}^+ + \text{Cl}^-$ with the following electron detachment of Cl^- . In Fig. 3 the temperature dependence of the stationary signals at the same probe voltage of $U = +50$ V is presented. Assuming, that the stationary probe signals ΔU_{st} (see Fig. 2) correspond to the state of the ionization equilibrium, the relation of concentrations of the electrons N_e , ions N_i and neutral atoms N_a must be described by the Saha equation:

$$\frac{N_e N_i}{N_a} = 2 \frac{Q_i}{Q_a} \left(\frac{2\pi \cdot m_e k T}{h^2} \right)^{3/2} \exp(-E_i / kT) \quad (1)$$

Here Q_a and Q_i are the partition functions for atoms and ions, m_e is the mass of electrons and E_i is the ionization potential of the given atoms.

The inset of Fig. 3 shows the same temperature dependence of measured signals in ‘‘Saha coordinates’’, assuming that $|\Delta U_{st}| \sim N_e$. The slope of this dependence fits well with the ionization potential of sodium $E_i(\text{Na}) = 5.14$ eV (dashed line). This fact finally

validates that sodium is the real source of the observed ionization. Based on this inference the equilibrium level of the electron concentration due to the ionization of sodium admixture was calculated. In Fig. 4 the calibration curve of the probe with a voltage of $U = +50$ V (electron probe), at the total sodium concentration equal to 2×10^{-5} % is shown.

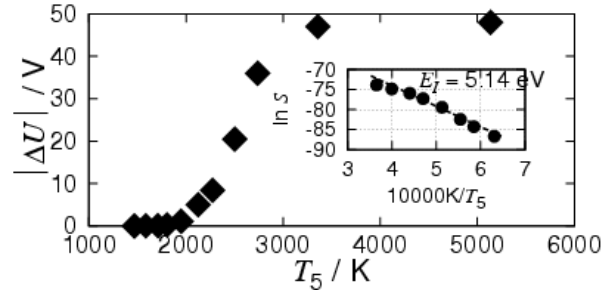


Fig. 3. Temperature dependence of the electron probe signal of $U = +50$ V. In the inset the same data as in the main plot, presented in ‘‘Saha coordinates’’:

$$S = (\Delta U_{st})^2 \frac{Q_a}{2N_a \cdot Q_i} \left(\frac{2\pi \cdot m_e k T}{h^2} \right)^{-3/2} \text{ are shown.}$$

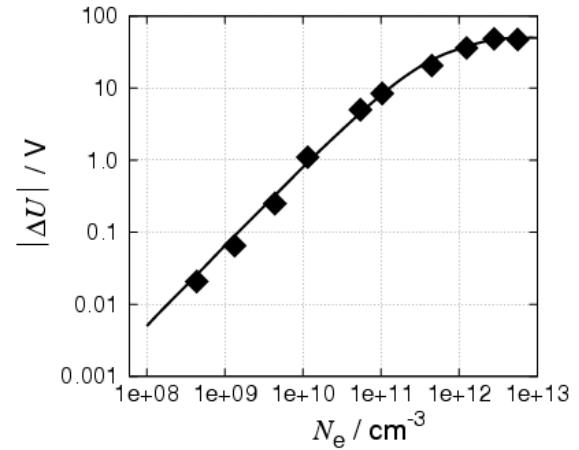


Fig. 4. Calibration curve for the electron probe at $U = +50$ V .

One can see that the given probe can be used to detect electron concentrations in the range of $(10^8 - 5 \cdot 10^{12}) \text{ cm}^{-3}$. The time resolution of these measurements depended on the probe size and the shock wave velocity and was varied in the range of $(1 - 2) \cdot 10^{-5}$ s. The accuracy of the measured electron concentration, caused by the uncertainty of the sodium content is about 50%.

The measurements at the probe with the negative voltage of $U = -50$ V (ion probe) did not show so stable signals. This is likely caused by the complicated processes of the ion drift in the ion probe sheath [25,26]. Therefore, the ion probe measurements were used for qualitative evaluation of the ion concentration behavior only.

Experimental results

Fig. 5 shows an example of the time profiles of laser extinction and signals from the positive and negative probes, measured in the mixture of 1% C_3O_2 in Ar at $T_5 = 2350$ K, $P_5 = 22$ bar. One can see from the extinction signal, that the particles are formed rather fast at times $t \sim 10^{-5}$ s and that they are stable during the whole measurement time. This observation coincides with the previous results of the rates of particle formation in the C_3O_2 pyrolysis [18]. The rise time of ion- and electron-probe signals show similar values of $\sim 3 \times 10^{-5}$ s, fitting with sodium ionization times (see calibration data above). However, in contrast to the experiments in Ar (see Fig. 2), both probe signals have a sharp maximum and a following decrease, which lasts for about 300 μ s. Measurements have shown that the magnitude of maximum signal on the ion probe is several times higher than the one measured in argon, while the electron probe signal appears to be several times less.

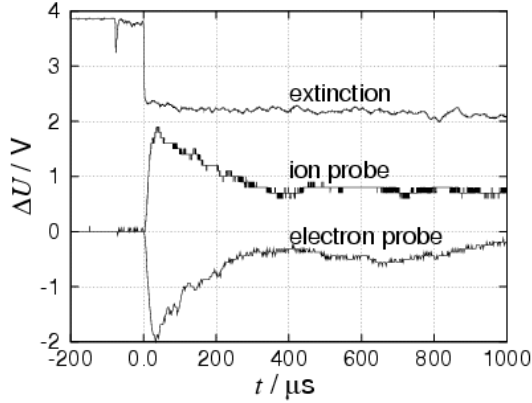


Fig. 5. Example of the time profile of laser extinction and signals from the positive and negative probes, measured in the mixture of 1% C_3O_2 in Ar at $T_5 = 2350$ K, $P_5 = 22$ bar.

In Fig. 6 the maximum electron and ion concentrations $N_{e(max)}$ and $N_{i(max)}$, registered by the probes at different temperatures and C_3O_2 concentrations are compared with the equilibrium electron and ion concentrations in argon calculated by the Saha equation (1) for sodium concentration $N_a = 2 \times 10^{-5}$ % [Ar] (shown by the upper line).

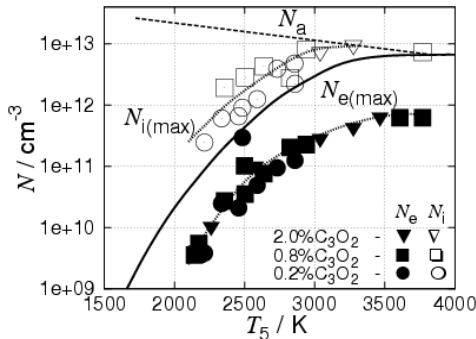


Fig. 6. Maximum electron and ion concentrations $N_{e(max)}$ and $N_{i(max)}$ registered by the probes at different temperatures and C_3O_2 content. The solid line is the equilibrium electron and ion concentrations in argon with the natural sodium admixture. The upper line shows the total Na concentration of $2 \cdot 10^{-5}$ % in Ar.

The adjustment to $N_{i(max)}$ values was based on the condition $N_{i(max)} \leq N_a$. The considerable deviation of both concentrations from the equilibrium curve (solid line) can be clearly observed. The magnitude of this deviation practically does not depend neither on temperature nor on C_3O_2 content. But it is remarkable that the product of $N_{e(max)}$ and $N_{i(max)}$ still closely agrees with the Saha values (1). Thus, already at these early times of $t \sim 10^{-5}$ s a large influence of the particles on electron and ion concentrations is observed.

The most interesting phenomenon, observed in these measurements is the decay of both electron and ion concentrations converting the complex plasma-particle system to the new equilibrium state. In Fig. 7 the final electron concentrations $N_{e(eq)}$ are given.

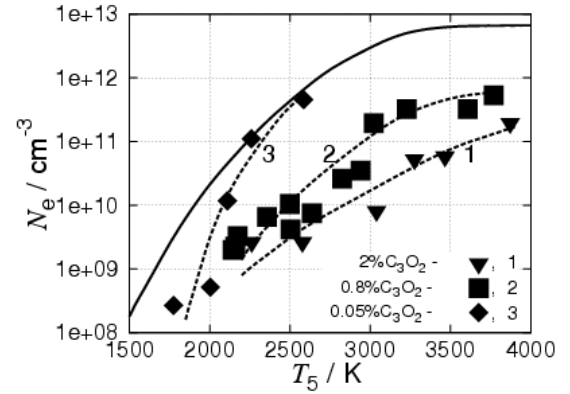


Fig. 7. Final electron concentrations $N_{e(eq)}$ measured at various particles concentrations. The solid line is the equilibrium electron concentration in argon with the natural admixture of sodium.

These values appear depending on the total concentration of carbon particles and in some cases they are about 100 times less than the initial electron concentrations, originating from the ionization of sodium. We do not give the quantitative values of $N_{i(eq)}$ because of the unreliability of the ion probe calibration during those measurements. However, qualitative measurements showed that the decay of ion concentrations is not so strong and the final N_i values are close to the initial ones $N_{i(eq)} \approx N_{i0}$.

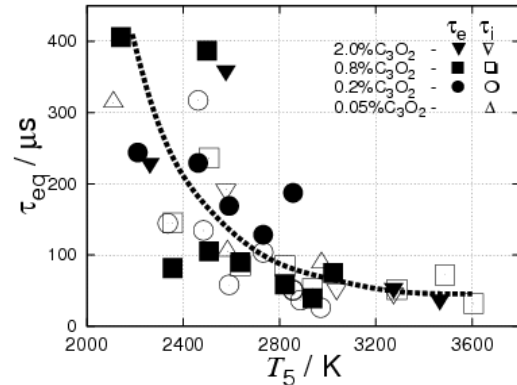


Fig. 8. Characteristic time of the establishment of the equilibrium τ_{eq} measured by both electron and ion probes using approximation (3). The dashed line is an estimation by $\tau_{eq} \sim N_{e0}^{-1/2}$ [27].

An important parameter, which could be extracted from the probe signal decay profiles, is the characteristic time of equilibrium establishment τ_{eq} . Assuming that the time profiles of both concentrations N_e and N_i (marked below as $N_{e(i)}$) can be described by the relaxation equation:

$$\frac{dN_{e(i)}}{dt} = \frac{N_{e(i)(eq)} - N_{e(i)}}{\tau_{eq}} \quad (2)$$

the effective values of τ_{eq} could be determined by the approximation of experimental data by the dependence

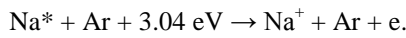
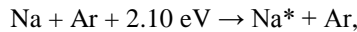
$$N_{e(i)} = N_{e(i)(max)} \exp(-t/\tau_{eq}) + N_{e(i)(eq)} (1 - \exp(-t/\tau_{eq})) \quad (3)$$

Fig. 8 gives the summary of all obtained data. Note, that both the electron and the ion probes show approximately the same τ_{eq} values independently on the C_3O_2 content. But the process of the approach of plasma-particle system to equilibrium displays a considerable acceleration with increasing temperature. This phenomenon seems to require an additional analysis.

Modeling and discussion

To analyse the obtained data on the time profiles of electron and ion concentrations, it is necessary to consider complex interrelation of the processes of: (a) free electrons and ions generation, which, is determined by the ionization of sodium atoms; (b) soot particles growth from the atomic carbon formed at the decomposition of molecules C_3O_2 ; (c) charging of these particles at recombination of electrons and ions on their surface.

For the description of the ionization kinetics the scheme of step-wise ionization of sodium atoms through an intermediate level $3p$ with energy of excitation 2.1 eV was applied:



As the rate constants of these reactions the values recommended in work [23] and extrapolated to the temperature range 2000 – 3500 K have been chosen:

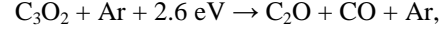
$$\alpha_1(T) = 5 \times 10^{-14} \exp(-24400/T), \text{ cm}^3\text{s}^{-1},$$

$$\alpha_2(T) = 1.4 \times 10^3 \frac{1}{T^3} \exp(-34300/T), \text{ cm}^3\text{s}^{-1}.$$

The used values of these constants well describe ionization in conditions of experiments [23] (5500 K < T < 8600 K), and in conditions of the given experiments as well.

The description of kinetic of soot particles formation includes the equations of decomposition of molecules C_3O_2 with formation of atomic carbon and the equations of soot particles growth as a result of sticking of carbon

atoms to their surface. For the description of this process it is necessary to set the concentration n_d of soot particles which is considered to be constant and equal to the concentration of the initial centers of the carbon nucleation. The values of these concentrations, depending on the temperature and volume fraction of C_3O_2 , have been taken from work [28]. Decomposition of molecules C_3O_2 includes the following reactions:

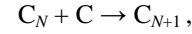


Rate constants of these reactions have been taken from [29]:

$$\alpha_3 = 2.4 \times 10^{-9} \exp(-29600/T), \text{ cm}^3\text{s}^{-1},$$

$$\alpha_4 = 1.4 \times 10^{-8} \exp(-29600/T), \text{ cm}^3\text{s}^{-1}.$$

Growth of soot particles is described by the scheme:



where N is quantity of carbon atoms in a particle. The rate constant of this reaction is obtained from the rate constants for particle size $N = 45$ given in [30] in assumption that it is proportional to cross-section of a particle, which, in turn, is proportional to $N^{2/3}$:

$$\alpha_5(N) = 3.5 \times 10^{-11} T^{1/2} (N/45)^{2/3}, \text{ cm}^3\text{s}^{-1}.$$

The process of soot particle formation in conditions of present experiments strongly influences on ionizing equilibrium in plasma, since recombination of ions and electrons on a particle susrface appears more intensive, than volumetric recombination of plasma. These processes are considered by addition components to the equations of plasma ionization:

$$\left(\frac{dn_e}{dt} \right)_{rec} = -\frac{n_e}{\tau_e}, \quad \left(\frac{dn_i}{dt} \right)_{rec} = -\frac{n_i}{\tau_i},$$

where n_e and n_i - concentrations of electrons and sodium ions. In the absence of a charge on the particles the ratio of characteristics time of electron and ion collisions with the particles (τ_e and τ_i) is inversely to their mobility K (in conditions of present experiments $K \approx 270$). Owing to larger mobility of electrons the soot particles get a negative charge, which partially inhibits the flux of electrons on the particle surface. This process is accounted by the factor $\exp(-Ze^2/aT)$ to the value of τ_e , reflecting the formation of a potential barrier for electrons. Here Z is the a charge of a particle in units of an electron charge ($Z < 0$) and a is the radius of a particle. The particle radius is connected with N by the ratio $(4/3)\pi a^3 = Nv_0$, where v_0 a volume on one atom of carbon ($v_0 \approx 10^{-23} \text{ cm}^3$). The particles charge Z is determined by the equation:

$$n_d \frac{dZ}{dt} = \frac{n_i}{\tau_i} - \frac{n_e}{\tau_{e0}} \exp(Ze^2/aT),$$

where τ_{e0} is the value τ_e for uncharged particle ($\tau_{e0} = \tau_i / K$), $\tau_i^{-1} = 4\pi n_d D_i a$ (D_i is the diffusion constant of ions).

The kinetic processes presented above are described by the system of six equations for plasma concentration, carbonaceous molecules, and also for the size and charge of soot particles.

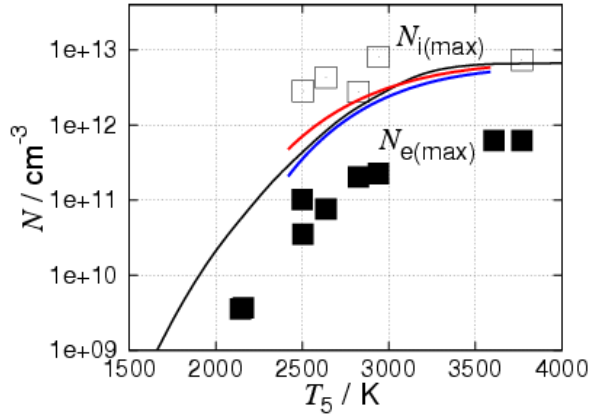


Fig. 9. The comparison of measured and calculated values of maximum electron and ion concentrations $N_{e(max)}$ and $N_{i(max)}$ in the mixture 0.8% $C_3O_2 + Ar$ at different temperatures. The black line is the equilibrium electron and ion concentrations in argon with the natural sodium admixture. The red and blue line is calculated maximum of ion and electron concentrations, correspondingly.

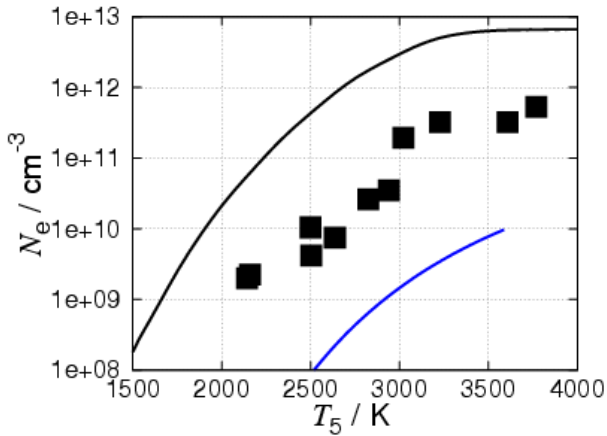


Fig. 10. The comparison of measured and calculated (blue line) values of final electron concentrations $N_{e(eq)}$ in the mixture 0.8% $C_3O_2 + Ar$. The black line is the equilibrium electron concentration in argon with the natural admixture of sodium.

Calculations have shown, that similar to experiments, concentrations of electrons and ions at presence of soot particles pass through a maximum. One can see that in the temperature range 2000 – 3000 K ion maximum concentration $N_{i(max)}$ is higher, than equilibrium concentration of plasma without soot, while electron maximum concentration $N_{e(max)}$ is lower (Fig.9). On the other hand the scale of calculated difference of $N_{i(max)}$ and $N_{e(max)}$ is much less than experimental data.

The calculated values of final electron concentrations also lie noticeably below experimental

values (Fig. 10) that can be connected with the incorrect accounting of the distribution function of particle size which is actually affected by coagulation, and with the approximate description of soot formation processes.

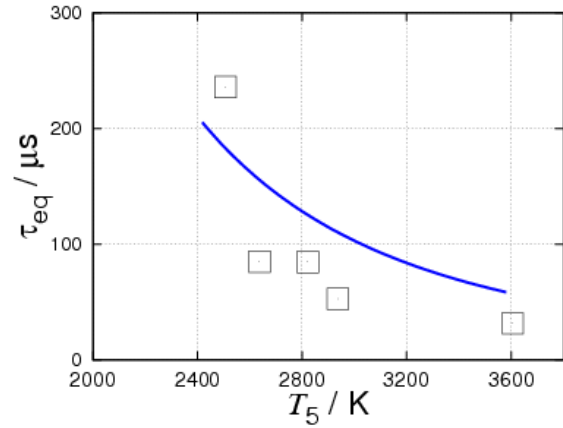


Fig. 11. Measured and calculated (blue line) characteristic times of the establishment of the equilibrium τ_{eq} in the mixture 0.8% $C_3O_2 + Ar$.

The calculated values of characteristic time of the equilibrium establishment show much better agreement with experimental results (Fig. 11). This fact evidently proves the correct accounting of the kinetics of the electron and ion fluxes to the particle surface at the latest stage of particle charging.

Conclusion

The electron and light ion concentrations originating from the natural sodium admixture in shock-heated gas are significantly modified in the presence of carbon particles.

Within $\sim 10^{-5}$ s after the shock front arrival the concentration of free electrons decreases by one order of magnitude, while the concentration of light positive ions increases by a factor of 5 – 7.

The time required for establishing the final equilibrium charge distribution varies from 400 to 40 μ s in the (2000 – 3600) K temperature and (15 – 30) bar pressure range.

The equilibrium concentration of free electrons in a particle-laden mixture is much less than in the same gas without particles and decreases proportionally to the square of the particle concentration.

The proposed modeling of the charging of particles in the process of their formation presents the satisfactory agreement of simulations with the experimental data. However, using only the value of mean particle size does not allow to attain quantitative agreement with experimental data on current and final electron and ion concentrations. Therefore further improvement of the modeling has to account the real distribution function of particle size

Acknowledgements

The support of this study by DFG, Göttingen Academy, Russian Academy of Sciences and RFBR is gratefully acknowledged.

References

- [1] B. S. Haynes, H. Jander, H. Gg. Wagner, *Proc. Combust. Inst.* 17 (1978) 1365-1374.
- [2] K. H. Homann, *Proc. Combust. Inst.* 20 (1986) 857-870.
- [3] A. Hospital, P. Roth, *Proc. Combust. Inst.* 2 (1990) 1573-1579.
- [4] M. M. Maricq, *Combust. Flame* 144 (2006) 730-743.
- [5] A. A. Onischuk, S. di Stasio, V. V. Karasev, et al., *J. Aerosol. Sci.* 34 (2003) 383-404.
- [6] E. Kovacevic, I. Stefanovic, J. Berndt, *J. Appl. Phys.* 93 (2003) 2924-2930.
- [7] M. A. Netleton, *J. Phys. D.* 5 (1972) L4-L6.
- [8] H. F. Calcote, *Combust. Flame* 42 (1981) 215-242.
- [9] Ph. Gerhardt, K. H. Homann, *J. Phys. Chem.* 94 (1990) 5381-5391.
- [10] M. Balthasar, F. Mauss, H. Wang, *Combust. Flame* 129 (2002) 204-216.
- [11] A. M. Savel'ev, A. M. Starik, *Tech. Phys.* 51 (2006) 444-452.
- [12] R. M. Moyerman, K. E. Shuler, *Science* 118 (1953) 612-614.
- [13] W. John, R. Kaifer, K. Rahn, J. Wesolowski, *J. Atmos. Environ.* 7 (1973) 107-111
- [14] G. S. Aravin, Yu. K. Karasevich, A. N. Shumeiko, *Combustion, Explosion and Shock Waves* 13 (1977) 611-618
- [15] A. Eremin, I. Naboko, S. Palopezhentsev, *Opt. Spektrosk.* 60 (1986) 920-927
- [16] J. Deppe, A. Emelianov, A. Eremin, H. Jander, H. Gg. Wagner, I. Zaslanko, *Proc. Combust. Inst.* 28 (2000) 2515-2522.
- [17] A. Emelianov, A. Eremin, H. Jander and H. Gg. Wagner, *Proc. Combust. Inst.* 29 (2002) 2351-2357.
- [18] A. Emelianov, A. Eremin, H. Jander, A. Makeich, P. Roth, R. Starke, H. Gg. Wagner, *Proc. Combust. Inst.* 30 (2004) 1433-1440.
- [19] A. Emelianov, A. Eremin, A. Makeich, H. Jander, H. Gg. Wagner, R. Starke, C. Schulz, *Proc. Combust. Inst.* 31 (2007) 649-656.
- [20] V. E. Fortov, A. G. Khrapak, S. A. Khrapak, V. I. Molotkov, O. F. Petrov, *Physics-Uspexhi* 47 (2004) 447-492.
- [21] V. N. Tsytovich, G. E. Morfill, and H. Thomas, *Plasma Phys. Rep.* 28 (2002) 623-651.
- [22] B. M. Smirnov, *Physics-Uspexhi* 43 (2000) 453 - 491.
- [23] K.-P. Schneider, C. Park, *Phys. Fluids* 18 (1975) 969-981.
- [24] S. Wang, J.-P. Cui, Y.-Z. He, B.-C. Fan, J. Wang, *Chin. Phys. Lett.* 18 (2001) 289-291.
- [25] P. R. Smy, *Adv. in Phys.* 25 (1976) 517 - 553.
- [26] I. Pollen, *Phys. Fluids* 7 (1964) 1433-1445.
- [27] A. Emelianov, A. Eremin, H. Jander, *Proc. Combust. Inst.* 32 (2009) 721-728.
- [28] J. Z. Wen, M. J. Thomson, M. F. Lightstone, *Combust. Theory and Modelling.* 10, 2, (2006), 257-272.
- [29] G. Friedrichs, H. Gg. Wagner, *Zeit. Phys. Chem.* 203, 1, (1998), 1-14.
- [30] A. Krestinin, A. Moravskij, P. Tesner, *Chem. Phys.* 17, 9, (1998), 70-84.